CRYSTALLOGRAPHIC COMMUNICATIONS

ISSN 2056-9890

Received 30 December 2025
Accepted 23 January 2026

Edited by J. Reibenspies, Texas A & M University, USA

Keywords: crystal structure; coumarin; trifluoromethanesulfonate-substituted.

CCDC reference: 2525434

Supporting information: this article has supporting information at journals.iucr.org/e

Crystal structure of 2-oxo-2*H*-chromen-7-yl trifluoromethanesulfonate

Navneet Goyal,[a]* Rafia Rashid,[a] Xiaodong Zhang,[b] Abha Verma,[a] Rami A. Al-Horani[c] and James P. Donahue[b]*

[a]Department of Chemistry, Xavier University of Louisiana, 1 Drexel Drive, New Orleans, LA 70125, USA, [b]Department of Chemistry, Tulane University, 6400 Freret Street, New Orleans, Louisiana 70118-5698, USA, and [c]Division of Basic Pharmaceutical Sciences, College of Pharmacy, Xavier University of Louisiana, 1 Drexel Drive, New Orleans, LA 70125, USA. *Correspondence e-mail: ngoyal@xula.edu, donahue@tulane.edu

Crystalline 2-oxo-2*H*-chromen-7-yl trifluoromethanesulfonate, $C_{10}H_5F_3O_5S$, forms in the monoclinic space group *C*2/*c* as pseudoplanar dyads about an inversion center, with close packing assisted by intermolecular C—H···O contacts of 2.38 Å. These dyads are arranged into a staircase pattern where the direction and pitch of the staircase are aligned with the *b* axis. Between adjacent stacks, molecules are related by a 2_1 axis and held in place by a herringbone-like network of additional intermolecular C—H···O contacts of 2.35 Å.

1. Chemical context

Hydroxy coumarins, such as 7-hydroxycoumarin (umbelliferone), are derivatives of common coumarin that posses hydroxyl groups, which enhance their solubility and biological activity (Kornicka *et al.*, 2023). These compounds find use in the detection of toxins such as cyanide (Eapen *et al.*, 2025), Hg^{2+} (Li *et al.*, 2020), and Pb^{2+} (Sharma & Gulati, 2021). They exhibit a broad spectrum of pharmacological properties, including antioxidant, anticoagulant, and antimicrobial activity, making them valuable in pharmaceutical research and applications (Kornicka *et al.*, 2023; Lee *et al.*, 2008).

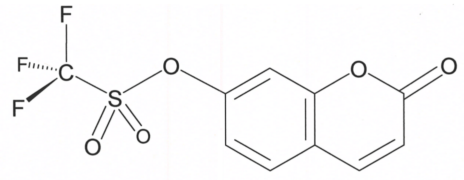

In synthetic organic chemistry, the hydroxy group of 7-hydroxycoumarin can be converted into an enhanced leaving group by reaction with triflic anhydride, thereby affording 2-oxo-2*H*-chromen-7-yl-trifluoromethanesulfonate, **I**. This triflate derivative is a highly activated electrophile, which can undergo cross-coupling (Zhang *et al.*, 2007) or nucleophilic substitution to install diverse substituents on the coumarin core (Grimm & Lavis, 2011), expanding the structural and functional diversity for pharmaceutical and agrochemical exploration and for development of fluorophore-based imaging agents (Otsuka *et al.*, 2016; López-Corrales *et al.*, 2023).

2. Structural commentary

Fig. 1(*a*) presents a view of 2-oxo-2*H*-chromen-7-yl-trifluoromethanesulfonate that is orthogonal to the coumarin ring

https://doi.org/10.1107/S205698902600071X

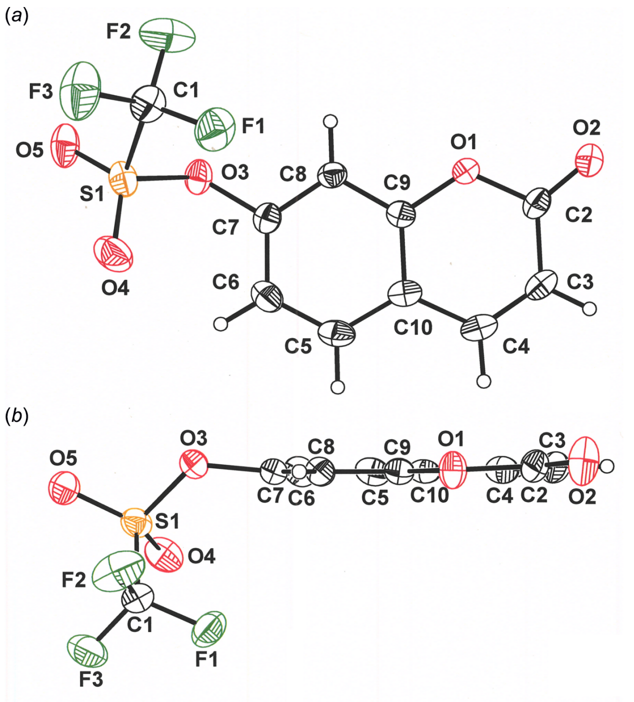

Figure 1
(*a*) Displacement ellipsoid plot (50% probability) of 2-oxo-2*H*-chromen-7-yl-trifluoromethanesulfonate, **I**, with complete atom labeling. (*b*) View of **I** along the edge of the coumarin plane. This perspective is from a position that is rotated by 90° from that shown in (*a*). Displacement ellipsoids are presented at the 50% probability level.

Table 1
Hydrogen-bond geometry (Å, °).

D—H⋯*A*	*D*—H	H⋯*A*	*D*⋯*A*	*D*—H⋯*A*
C3—H3⋯O2^{i}	0.95	2.35	3.267 (2)	162
C8—H8⋯O2^{ii}	0.95	2.38	3.293 (2)	162

Symmetry codes: (i) $-x+\frac{3}{2}, y+\frac{1}{2}, -z+\frac{1}{2}$; (ii) $-x+\frac{3}{2}, -y+\frac{1}{2}, -z+1$.

system, with atom labeling in accord with the IUPAC numbering system (Annunziata *et al.*, 2020). The eleven atoms of the coumarin ring system are planar with a mean deviation of 0.021 Å. The maximum out-of-plane deviation is shown by O1 [0.039 (1) Å], as it is the only exocyclic atom of the parent structure. As seen in Fig. 1(*b*), O3 is bent slightly, but discernibly [0.173 (1) Å], to the upper face of the coumarin plane, while the triflate substituent as a whole is oriented downward toward the opposite (bottom) face. The C7—O3—S1—C1 torsion angle is 81.57 (15)°. The interatomic distances within the coumarin core of **I** are the same, within experimental resolution, as those observed in $P2_1$ (Zhang *et al.*, 2021) and $Pca2_1$ (Waddell *et al.*, 2024) polymorphs of coumarin itself.

3. Supramolecular features

The extended packing pattern of 2-oxo-2*H*-chromen-7-yl-trifluoromethanesulfonate molecules begins with pseudo-coplanar pairs disposed around an inversion center and held in place, in part, via C8—H8⋯O2 close contacts of 2.38 Å (Table 1, Fig. 2). These dyads are arranged in a staircase-like fashion that places the top face of the coumarin ring system of one dyad member into a π–π stacking interaction with the step above, while the bottom face of its centrosymmetric partner is similarly related to the dyad that forms the step below (Fig. 3). The π–π stacks are also formed around inversion centers,

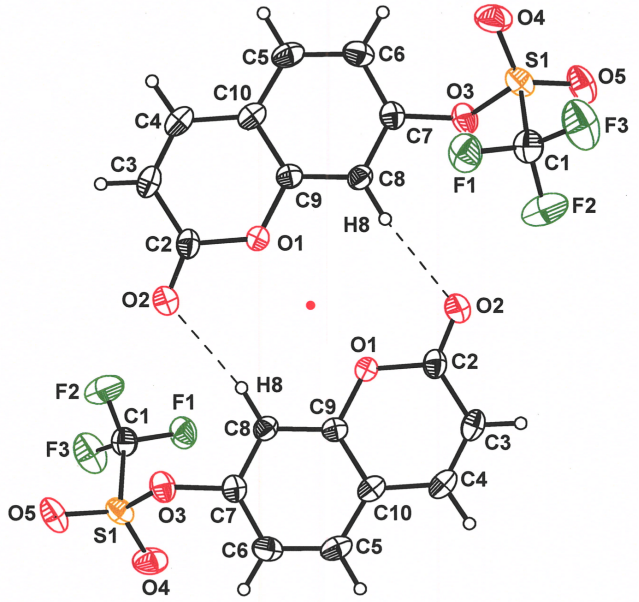

Figure 2
Pseudoplanar dyads of **I** formed by pairwise C8—H8⋯O2 interactions across an inversion center. The position of the inversion center is marked with a red point. Displacement ellipsoids are shown at 50%.

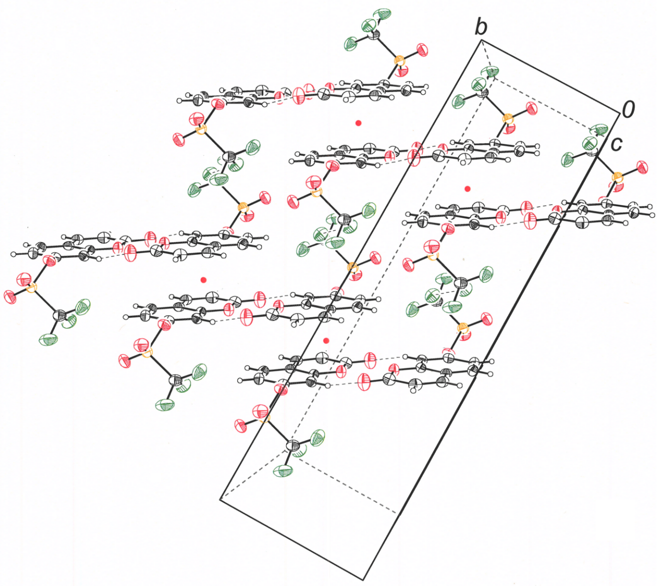

Figure 3
View down the *c* axis of the cell showing the staircase-like arrangement of dyads of **I** along the *b* axis of the cell. Displacement ellipsoids are drawn at the 50% probability level. Red points designate the positions of inversion centers that relate each step of the staircase to its symmetry partners above and below. Displacement ellipsoids are drawn at the 50% level.

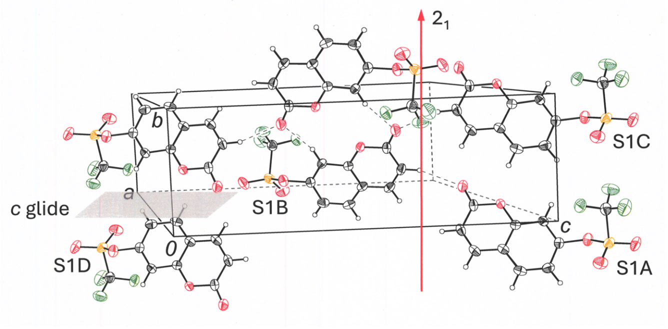

Figure 4
Partial packing of the unit cell for **I** showing molecules related by 2_1 symmetry and by the *c* glide operation. Displacement ellipsoids are shown at 50%.

marked as red points in Fig. 3, a consequence of which is that the coumarin rings of different steps approach one another in a tail-to-tail manner but with a sideways slip that places carbon 9 of one molecule above carbon 9 of its partner at a separation of 3.443 (2) Å. This distance is well within the 3.3-3.8 Å that is regarded as typical of offset parallel planar aromatic ring interactions (Janiak, 2000). The stair-like formations of dyads lie in the *ab* plane of the unit cell, with the *b* axis defining both the direction and the pitch of the staircase (Fig. 3).

Between the staircase-like stacks of molecules on the *ab* faces of the cell lie other stacks to which they are related by 2_1 axes. Fig. 4 illustrates how the molecule bearing the S1B label is related by a 2_1 axis in red to the molecules with the S1A and S1C labels. Similarly, this same molecule is related to the molecule with the S1D label by a *c* glide plane (in gray), which is parallel to the *ac* plane and orthogonal to the *b* axis (Fig. 4). A consequence of the positioning of 2_1 axis between adjacent stacks is that the coumarin molecular planes in adjoining stacks have the same angular disposition of 26° relative to the stacking axis but in opposite directions (Fig. 5). Thus, when these stacks are considered from the perspective along the stacking axis, molecules similarly eclipse one another without giving clear evidence of the alternating angle of cant between them (Fig. 6). Close contacts of 2.35 Å between C3–H3$\cdots$O2 form the predominant interstack interactions (Table 1, Fig. 5). Although F1$\cdots$F1 intermolecular contacts of 2.863 (2) Å do occur (not illustrated), which is less than the 3.00 Å sum of the crystallographic van der Waals radii (Batsanov, 2001), the 139.97° C—F$\cdots$F angle places this interaction into the Type I category of nonstabilizing F$\cdots$F interactions that is driven by the larger packing pattern (Reichenbächer *et al.*, 2005).

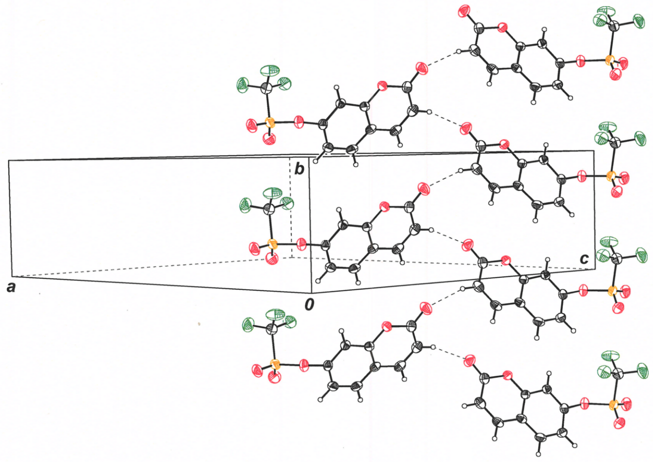

Figure 5
View approximately along the *ac* face diagonal of the cell showing adjacent molecular stacks in the direction of the *b* axis. Intermolecular C3—H3$\cdots$O2 close contacts are illustrated with dashed lines. Displacement ellipsoids are drawn at the 50% level.

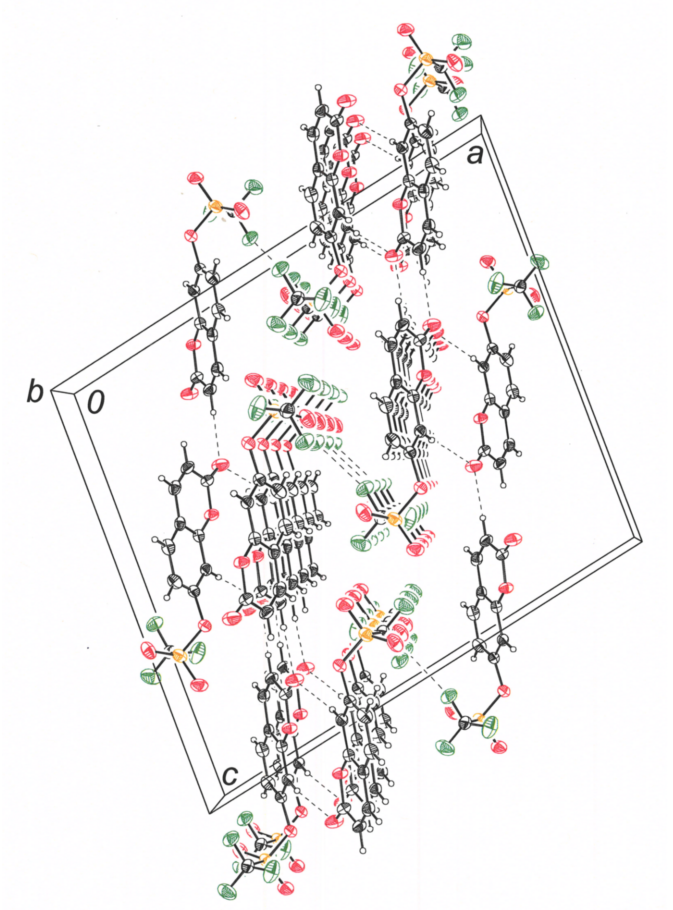

Figure 6
View down the *b* axis of the cell showing eclipsed columnar stacks of **I**. Displacement ellipsoids are shown at 50%.

4. Database survey

Related molecules that have been identified structurally by X-ray crystallography are 4-trifluoromethyl-7-trifluoromethanesulfonato-2*H*-chromen-2-one (Qin *et al.*, 2025), 6,7-bis(trifluoromethanesulphonato)-4-methyl-2*H*-chromen-2-one (Hamdy *et al.*, 2016), 7-(4-methoxyphenyl)-4-methyl-6-trifluoromethanesulphonato-2*H*-chromen-2-one (Hamdy *et al.*, 2016), and 6,7-bis(trifluoromethanesulfonato)-3-bromo-4-methyl-2-oxo-2*H*-chromene (Hamdy *et al.*, 2016).

5. Synthesis and crystallization

The starting material, 7-hydroxycoumarin (0.500 g, 3.08 mmol) was dissolved in dry THF (25 ml) under an N_2 atmosphere and cooled to 273 K. Triethylamine (1.1 ml, 7.70 mmol) was added to the reaction mixture. After stirring for 15 min at 273 K, triflic anhydride (0.57 ml, 3.39 mmol) was added dropwise. The reaction mixture was stirred at ambient temperature for 2 h, and progress of the reaction was monitored using thin-layer chromatography (TLC). The reaction mixture was extracted with EtOAc (50 ml) and H_2O (25 ml). The organic layer was separated and dried over anyhdrous sodium sulfate. The solvent was evaporated under vacuum, and the crude product was purified by flash column chromatography on silica gel using 1:3 EtOAc:hexanes (*v*/*v*) as the eluant to yield the target compound as a white solid (0.810 g, 90% yield). Crystals were obtained by slow cooling of a warm solution in 2:1 EtOAc:hexanes (*v*/*v*). ^{1}H NMR (300 MHz, δ, p.p.m. in $CDCl_3$): 6.50 (*d*, $J = 9.6$ Hz, 1 H), 7.22–7.26 (*m*, 1 H), 7.27–7.30 (*m*, 1 H), 7.61 (*d*, $J = 8.4$ Hz, 1 H), 7.74 (*d*, $J = 9.6$ Hz, 1 H). ^{13}C NMR (75 MHz, δ, p.p.m. in $CDCl_3$): 110.5, 117.7, 177.8, 188.8, 120.3, 129.5, 142.1, 150.8, 154.6, 159.3.

6. Refinement

Crystal data, data collection and structure refinement details are summarized in Table 2. Hydrogen atoms were added in calculated positions and refined with isotropic displacement parameters that were approximately 1.2 times (for aromatic C—H) those of the carbon atoms to which they were attached. The C—H distance assumed was 0.95 Å.

Table 2
Experimental details.

Crystal data	
Chemical formula	$C_{10}H_5F_3O_5S$
M_r	294.20
Crystal system, space group	Monoclinic, *C*2/*c*
Temperature (K)	150
a, *b*, *c* (Å)	20.4767 (9), 6.0828 (3), 18.2181 (8)
β (°)	102.137 (2)
V (Å^3)	2218.45 (18)
Z	8
Radiation type	Mo *K*α
μ (mm^{-1})	0.35
Crystal size (mm)	0.17 × 0.06 × 0.03
Data collection	
Diffractometer	Bruker D8
Absorption correction	Multi-scan (*SADABS*; Krause *et al.*, 2015)
T_{min}, T_{max}	0.927, 0.988
No. of measured, independent and observed [$I > 2\sigma(I)$] reflections	28942, 3542, 2127
R_{int}	0.069
$(\sin \theta/\lambda)_{max}$ (Å^{-1})	0.725
Refinement	
$R[F^2 > 2\sigma(F^2)]$, $wR(F^2)$, *S*	0.044, 0.107, 1.04
No. of reflections	3542
No. of parameters	172
H-atom treatment	H-atom parameters constrained
$\Delta\rho_{max}$, $\Delta\rho_{min}$ (e Å^{-3})	0.35, −0.37

Computer programs: *APEX5* and *SAINT* (Bruker, 2024), *SHELXT2018/2* (Sheldrick, 2015*a*), *SHELXL2019/2* (Sheldrick, 2015*b*) and *SHELXTL* (Sheldrick, 2008).

Funding information

This work was supported by the Institutional Development Award (IDeA) from the National Institute of General Medical Sciences of the National Institutes of Health under grant No. P20GM103424-21, by the National Institute of General Medical Sciences of the National Institutes of Health under award No. R16GM149412, and by the National Science Foundation under award No. NSF-2315727 in collaboration with Professor Dorin Boldor of Louisiana State University. The National Science Foundation (MRI: 1228232) is thanked for funding the purchase of Tulane University's Bruker D8 Quest diffractometer with Photon 3 CPAD detector and for support of this project (CHE: 1836589). Tulane University is acknowledged for its ongoing assistance with operational costs for its X-ray diffraction facility.

References

Annunziata, F., Pinna, C., Dallavalle, S., Tamborini, L. & Pinto, A. (2020). *Int. J. Mol. Sci.* **21**, 4618.
Batsanov, S. S. (2001). *Inorg. Mater.* **37**, 871–885.
Bruker (2024). *APEX5* and *SAINT*. Bruker AXS Inc., Madison, Wisconsin, USA.
Eapen, A. K., Das, D., Sutradhar, S., Sarkar, P. & Ghosh, B. N. (2025). *J. Mol. Struct.* **1337**, 142188.
Grimm, J. B. & Lavis, L. D. (2011). *Org. Lett.* **13**, 6354–6357.
Hamdy, A. M., Khaddour, Z., Al-Masoudi, N. A., Rahman, Q., Hering-Junghans, C., Villinger, A. & Langer, P. (2016). *Bioorg. Med. Chem.* **24**, 5115–5126.
Janiak, C. (2000). *J. Chem. Soc. Dalton Trans.* pp. 3885–3896.
Kornicka, A., Balewski, L., Lahutta, M. & Kokoszka, J. (2023). *Pharmaceuticals* **16**, 1732.
Krause, L., Herbst-Irmer, R., Sheldrick, G. M. & Stalke, D. (2015). *J. Appl. Cryst.* **48**, 3–10.
Lee, K.-S., Kim, H.-J., Kim, G.-H., Shin, I. & Hong, J.-I. (2008). *Org. Lett.* **10**, 49–51.
Li, X., Duan, Q., Yu, Y., Wang, K., Zhu, H., Zhang, X., Liu, C., Jia, P., Li, Z., Sheng, W. & Zhu, B. (2020). *Luminescence* **35**, 941–946.
López-Corrales, M., Rovira, A., Gandioso, A., Nonell, S., Bosch, M. & Marchán, V. (2023). *J. Org. Chem.* **88**, 7128–7140.
Otsuka, Y., Sasaki, A., Teshima, T., Yamada, K. & Yamamoto, T. (2016). *Org. Lett.* **18**, 1338–1341.
Qin, X., Li, Y., Song, R., Wang, L. & Ye, B. (2025). *Z. Kristallogr. New Cryst. Struct.* **240**, 523–526.
Reichenbächer, K., Süss, K. I. & Hulliger, J. (2005). *Chem. Soc. Rev.* **34**, 22–30.
Sharma, N. & Gulati, A. (2021). *Luminescence* **36**, 1172–1180.
Sheldrick, G. M. (2008). *Acta Cryst.* A**64**, 112–122.
Sheldrick, G. M. (2015*a*). *Acta Cryst.* A**71**, 3–8.
Sheldrick, G. M. (2015*b*). *Acta Cryst.* C**71**, 3–8.
Waddell, P. G., Probert, M. R. & Johnson, N. T. (2024). *J. Chem. Educ.* **101**, 4276–4281.
Zhang, K., Sun, C. C., Liu, Y., Wang, C., Shi, P., Xu, J., Wu, S. & Gong, J. (2021). *Chem. Mater.* **33**, 1053–1060.
Zhang, L., Meng, T., Fan, R. & Wu, J. (2007). *J. Org. Chem.* **72**, 7279–7286.

supporting information

Acta Cryst. (2026). E**82**, 227-230 [https://doi.org/10.1107/S205698902600071X]

Crystal structure of 2-oxo-2*H*-chromen-7-yl trifluoromethanesulfonate

Navneet Goyal, Rafia Rashid, Xiaodong Zhang, Abha Verma, Rami A. Al-Horani and James P. Donahue

Computing details

2-Oxo-2*H*-chromen-7-yl trifluoromethanesulfonate

Crystal data

$C_{10}H_5F_3O_5S$	$F(000) = 1184$
$M_r = 294.20$	$D_x = 1.762$ Mg m^{-3}
Monoclinic, $C2/c$	Mo $K\alpha$ radiation, $\lambda = 0.71073$ Å
$a = 20.4767$ (9) Å	Cell parameters from 4023 reflections
$b = 6.0828$ (3) Å	$\theta = 3.4–25.5°$
$c = 18.2181$ (8) Å	$\mu = 0.35$ mm^{-1}
$\beta = 102.137$ (2)°	$T = 150$ K
$V = 2218.45$ (18) Å^3	Block, colorless
$Z = 8$	0.17 × 0.06 × 0.03 mm

Data collection

Bruker D8 diffractometer	28942 measured reflections
Radiation source: sealed tube	3542 independent reflections
Flat graphite monochromator	2127 reflections with $I > 2\sigma(I)$
Detector resolution: 7.391 pixels mm^{-1}	$R_{int} = 0.069$
ω and φ scans	$\theta_{max} = 31.0°$, $\theta_{min} = 2.3°$
Absorption correction: multi-scan (*SADABS*; Krause *et al.*, 2015)	$h = -29 \rightarrow 29$
	$k = -8 \rightarrow 8$
$T_{min} = 0.927$, $T_{max} = 0.988$	$l = -26 \rightarrow 26$

Refinement

Refinement on F^2	Hydrogen site location: inferred from neighbouring sites
Least-squares matrix: full	H-atom parameters constrained
$R[F^2 > 2\sigma(F^2)] = 0.044$	$w = 1/[\sigma^2(F_o^2) + (0.0376P)^2 + 1.1073P]$ where $P = (F_o^2 + 2F_c^2)/3$
$wR(F^2) = 0.107$	$(\Delta/\sigma)_{max} = 0.001$
$S = 1.04$	$\Delta\rho_{max} = 0.35$ e Å^{-3}
3542 reflections	$\Delta\rho_{min} = -0.37$ e Å^{-3}
172 parameters	
0 restraints	
Primary atom site location: intrinsic phasing	

Special details

Geometry. All esds (except the esd in the dihedral angle between two l.s. planes) are estimated using the full covariance matrix. The cell esds are taken into account individually in the estimation of esds in distances, angles and torsion angles; correlations between esds in cell parameters are only used when they are defined by crystal symmetry. An approximate (isotropic) treatment of cell esds is used for estimating esds involving l.s. planes.

Fractional atomic coordinates and isotropic or equivalent isotropic displacement parameters (Å²)

	x	y	z	$U_{\rm iso}$*/$U_{\rm eq}$
S1	0.56456 (2)	0.72261 (8)	0.66170 (3)	0.03075 (14)
F1	0.52714 (6)	0.3963 (2)	0.57032 (6)	0.0431 (3)
F2	0.58390 (7)	0.3006 (2)	0.67780 (8)	0.0543 (4)
F3	0.48224 (7)	0.4049 (2)	0.66635 (8)	0.0565 (4)
O1	0.71324 (6)	0.4339 (2)	0.43122 (7)	0.0282 (3)
O2	0.76131 (8)	0.2925 (2)	0.34462 (8)	0.0412 (4)
O3	0.63257 (6)	0.7226 (2)	0.63519 (7)	0.0308 (3)
O4	0.51608 (7)	0.8532 (2)	0.61494 (9)	0.0426 (4)
O5	0.58160 (7)	0.7476 (2)	0.74031 (8)	0.0406 (4)
C1	0.53785 (10)	0.4375 (3)	0.64313 (11)	0.0322 (5)
C2	0.72999 (10)	0.4453 (3)	0.36176 (10)	0.0291 (4)
C3	0.70878 (10)	0.6384 (3)	0.31694 (11)	0.0316 (4)
H3	0.718411	0.649575	0.268294	0.038*
C4	0.67597 (9)	0.8014 (3)	0.34233 (11)	0.0306 (4)
H4	0.662584	0.926352	0.311571	0.037*
C5	0.62832 (10)	0.9553 (3)	0.44742 (12)	0.0322 (5)
H5	0.614123	1.084405	0.419228	0.039*
C6	0.61648 (10)	0.9353 (3)	0.51895 (12)	0.0324 (5)
H6	0.594656	1.048660	0.540455	0.039*
C7	0.63747 (9)	0.7445 (3)	0.55832 (10)	0.0258 (4)
C8	0.66927 (9)	0.5751 (3)	0.53042 (10)	0.0248 (4)
H8	0.682938	0.446113	0.558939	0.030*
C9	0.68042 (8)	0.6017 (3)	0.45848 (10)	0.0239 (4)
C10	0.66065 (9)	0.7901 (3)	0.41557 (11)	0.0262 (4)

Atomic displacement parameters (Å²)

	U^{11}	U^{22}	U^{33}	U^{12}	U^{13}	U^{23}
S1	0.0284 (3)	0.0301 (3)	0.0362 (3)	−0.0015 (2)	0.0125 (2)	−0.0065 (2)
F1	0.0539 (8)	0.0436 (7)	0.0294 (7)	−0.0069 (6)	0.0033 (6)	−0.0088 (6)
F2	0.0619 (9)	0.0329 (7)	0.0562 (9)	0.0004 (6)	−0.0148 (7)	0.0039 (6)
F3	0.0522 (8)	0.0631 (9)	0.0614 (9)	−0.0282 (7)	0.0284 (7)	−0.0191 (7)
O1	0.0372 (8)	0.0259 (7)	0.0233 (7)	0.0058 (6)	0.0103 (6)	0.0042 (6)
O2	0.0562 (10)	0.0418 (9)	0.0283 (8)	0.0135 (7)	0.0153 (7)	0.0012 (7)
O3	0.0243 (7)	0.0407 (8)	0.0289 (8)	−0.0015 (6)	0.0088 (6)	−0.0029 (6)
O4	0.0313 (8)	0.0391 (9)	0.0596 (11)	0.0098 (7)	0.0142 (7)	0.0059 (7)
O5	0.0439 (9)	0.0466 (9)	0.0349 (9)	−0.0097 (7)	0.0166 (7)	−0.0173 (7)
C1	0.0309 (11)	0.0362 (11)	0.0284 (11)	−0.0047 (9)	0.0034 (9)	−0.0028 (9)
C2	0.0306 (10)	0.0363 (11)	0.0198 (10)	−0.0003 (9)	0.0042 (8)	0.0008 (8)

C3	0.0342 (11)	0.0381 (11)	0.0209 (10)	−0.0031 (9)	0.0024 (8)	0.0061 (9)
C4	0.0284 (10)	0.0308 (10)	0.0298 (11)	−0.0042 (8)	−0.0003 (8)	0.0103 (8)
C5	0.0291 (10)	0.0237 (10)	0.0429 (13)	0.0000 (8)	0.0056 (9)	0.0083 (9)
C6	0.0313 (11)	0.0252 (10)	0.0424 (13)	0.0019 (8)	0.0119 (9)	−0.0014 (9)
C7	0.0223 (9)	0.0302 (10)	0.0250 (10)	−0.0028 (8)	0.0055 (8)	−0.0011 (8)
C8	0.0232 (9)	0.0259 (10)	0.0249 (10)	0.0018 (7)	0.0043 (8)	0.0044 (8)
C9	0.0212 (9)	0.0234 (9)	0.0265 (10)	−0.0002 (7)	0.0037 (7)	0.0005 (8)
C10	0.0210 (9)	0.0255 (9)	0.0298 (10)	−0.0036 (7)	0.0002 (8)	0.0056 (8)

Geometric parameters (Å, º)

S1—O5	1.4092 (15)	C3—H3	0.9500
S1—O4	1.4094 (15)	C4—C10	1.435 (3)
S1—O3	1.5671 (13)	C4—H4	0.9500
S1—C1	1.829 (2)	C5—C6	1.380 (3)
F1—C1	1.322 (2)	C5—C10	1.395 (3)
F2—C1	1.316 (2)	C5—H5	0.9500
F3—C1	1.310 (2)	C6—C7	1.384 (3)
O1—C9	1.372 (2)	C6—H6	0.9500
O1—C2	1.381 (2)	C7—C8	1.372 (3)
O2—C2	1.207 (2)	C8—C9	1.386 (2)
O3—C7	1.431 (2)	C8—H8	0.9500
C2—C3	1.444 (3)	C9—C10	1.398 (2)
C3—C4	1.334 (3)		
O5—S1—O4	123.08 (9)	C3—C4—H4	119.6
O5—S1—O3	105.48 (8)	C10—C4—H4	119.6
O4—S1—O3	111.86 (8)	C6—C5—C10	121.48 (18)
O5—S1—C1	106.92 (9)	C6—C5—H5	119.3
O4—S1—C1	106.11 (10)	C10—C5—H5	119.3
O3—S1—C1	101.16 (8)	C5—C6—C7	117.77 (18)
C9—O1—C2	121.96 (14)	C5—C6—H6	121.1
C7—O3—S1	123.46 (11)	C7—C6—H6	121.1
F3—C1—F2	109.46 (18)	C8—C7—C6	123.88 (17)
F3—C1—F1	108.86 (16)	C8—C7—O3	115.41 (16)
F2—C1—F1	108.22 (17)	C6—C7—O3	120.45 (16)
F3—C1—S1	109.27 (14)	C7—C8—C9	116.58 (17)
F2—C1—S1	110.80 (13)	C7—C8—H8	121.7
F1—C1—S1	110.20 (14)	C9—C8—H8	121.7
O2—C2—O1	116.49 (17)	O1—C9—C8	116.47 (15)
O2—C2—C3	126.38 (18)	O1—C9—C10	120.92 (16)
O1—C2—C3	117.13 (17)	C8—C9—C10	122.60 (17)
C4—C3—C2	121.47 (18)	C5—C10—C9	117.68 (17)
C4—C3—H3	119.3	C5—C10—C4	124.61 (17)
C2—C3—H3	119.3	C9—C10—C4	117.70 (17)
C3—C4—C10	120.76 (18)		
O5—S1—O3—C7	−167.17 (14)	C5—C6—C7—C8	0.1 (3)

O4—S1—O3—C7	−31.00 (16)	C5—C6—C7—O3	173.90 (17)
C1—S1—O3—C7	81.57 (15)	S1—O3—C7—C8	−121.98 (16)
O5—S1—C1—F3	66.41 (16)	S1—O3—C7—C6	63.7 (2)
O4—S1—C1—F3	−66.57 (16)	C6—C7—C8—C9	0.1 (3)
O3—S1—C1—F3	176.56 (13)	O3—C7—C8—C9	−173.99 (15)
O5—S1—C1—F2	−54.27 (17)	C2—O1—C9—C8	−176.98 (16)
O4—S1—C1—F2	172.75 (14)	C2—O1—C9—C10	2.0 (3)
O3—S1—C1—F2	55.87 (16)	C7—C8—C9—O1	178.91 (15)
O5—S1—C1—F1	−174.02 (13)	C7—C8—C9—C10	0.0 (3)
O4—S1—C1—F1	53.00 (16)	C6—C5—C10—C9	0.4 (3)
O3—S1—C1—F1	−63.87 (15)	C6—C5—C10—C4	−178.56 (18)
C9—O1—C2—O2	176.94 (16)	O1—C9—C10—C5	−179.14 (16)
C9—O1—C2—C3	−2.8 (2)	C8—C9—C10—C5	−0.2 (3)
O2—C2—C3—C4	−177.9 (2)	O1—C9—C10—C4	−0.1 (3)
O1—C2—C3—C4	1.7 (3)	C8—C9—C10—C4	178.84 (17)
C2—C3—C4—C10	0.1 (3)	C3—C4—C10—C5	178.07 (19)
C10—C5—C6—C7	−0.4 (3)	C3—C4—C10—C9	−0.9 (3)

Hydrogen-bond geometry (Å, º)

D—H···*A*	*D*—H	H···*A*	*D*···*A*	*D*—H···*A*
C3—H3···O2^{i}	0.95	2.35	3.267 (2)	162
C8—H8···O2^{ii}	0.95	2.38	3.293 (2)	162

Symmetry codes: (i) −*x*+3/2, *y*+1/2, −*z*+1/2; (ii) −*x*+3/2, −*y*+1/2, −*z*+1.